

SCIENTIFIC REPORTS

OPEN

Calcium and vitamin-D deficiency marginally impairs fracture healing but aggravates posttraumatic bone loss in osteoporotic mice

Verena Fischer¹, Melanie Haffner-Luntzer¹, Katja Prystaz¹, Annika vom Scheidt², Björn Busse², Thorsten Schinke², Michael Amling² & Anita Ignatius¹

Calcium and vitamin-D (Ca/VitD) deficiency is a major risk factor for osteoporosis. It may also contribute to the compromised bone healing frequently observed in osteoporotic patients, since calcium is essential for fracture-callus mineralization. Additionally, clinical data suggest systemic bone loss following fracture, which may aggravate osteoporosis and thus increase the risk for fragility fractures in osteoporotic patients further. However, the role of Ca/VitD in fracture healing and posttraumatic bone turnover has to date been poorly investigated. Here, we studied bone regeneration and posttraumatic bone turnover in C57BL/6J mice with ovariectomy-induced osteoporosis. Mice were fed a standard or a Ca/VitD-deficient diet. Notably, fracture healing was only marginally disturbed in Ca/VitD-deficient mice. However, deficient mice displayed significantly increased serum parathyroid hormone levels and osteoclast activity, as well as reduced bone mass in the intact skeleton post-fracture, suggesting considerably enhanced calcium mobilization from the intact skeleton during bone regeneration. Ca/VitD supplementation initiated post-fracture prevented posttraumatic bone loss by reducing bone resorption and furthermore improved bone repair. These results imply that adequate Ca/VitD supply post-fracture is essential to provide sufficient calcium for callus-mineralization in order to prevent posttraumatic bone loss and to reduce the risk for secondary fractures in osteoporotic patients with Ca/VitD deficiency.

Osteoporosis is the most common skeletal disorder worldwide and is associated with a progressive decline in bone properties and an increased fracture risk. Calcium and vitamin-D (Ca/VitD) deficiency is a major risk factor for osteoporosis in addition to postmenopausal estrogen decline, old age and immobilization¹. Vitamin D regulates calcium homeostasis by influencing intestinal calcium absorption, renal calcium reabsorption and bone resorption by osteoclasts². Both vitamin-D deficiency and a low calcium supply result in increased bone resorption to maintain blood calcium, thus reducing bone mass and quality^{3,4}. It is estimated that approximately 3 billion people worldwide display vitamin-D deficiency⁵. Due to on-going demographic changes, the number is expected to increase, because in the elderly dietary calcium and vitamin-D intake are mostly insufficient and intestinal calcium absorption and endogenous vitamin-D synthesis are reduced^{6–8}. Therefore, to prevent osteoporosis, the National Osteoporosis Foundation recommends Ca/VitD supplementation for individuals at a high risk for osteoporosis, including postmenopausal females aged over 50 with inadequate dietary calcium and vitamin-D intake⁹. However, osteoporosis is frequently undiagnosed until patients have experienced the first fragility fracture and even after fracture, 80–90% of patients do not receive adequate treatment^{10,11}. Concluding, even though a sufficient Ca/VitD supply is crucial for skeletal health, undersupply is common, particularly in the osteoporotic elderly^{12,13}.

Furthermore, Ca/VitD deficiency may also contribute to fracture-healing complications that are frequently observed in osteoporotic patients^{14,15}, because calcium is essential for fracture-callus mineralization^{16,17}. Notably, the role of calcium and vitamin D in fracture healing has to date been poorly investigated. There are a limited number of conflicting experimental studies reporting either a negative^{18,19} or no effect²⁰ of Ca/VitD deficiency

¹Institute of Orthopaedic Research and Biomechanics, University Medical Centre Ulm, Ulm, Germany. ²Department of Osteology and Biomechanics, University Medical Centre Hamburg-Eppendorf, Hamburg, Germany. Correspondence and requests for materials should be addressed to A.I. (email: anita.ignatius@uni-ulm.de)

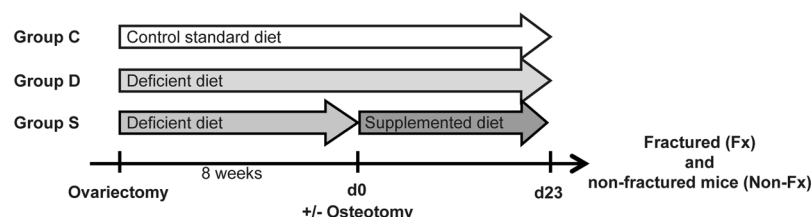


Figure 1. Study design. Following ovariectomy of female C57BL/6 J mice (aged 18 weeks), mice of group C were fed a standard control diet and mice of groups D and S a Ca/VitD-deficient diet. After 8 weeks, mice received a femur osteotomy and group S was transferred to a Ca/VitD-supplemented diet post-fracture. Mice were sacrificed 10 and 23 days after osteotomy. Bone turnover in the intact skeleton of fractured mice (Fx) was compared to that of ovariectomized non-fractured mice (Non-Fx), which received the same feeds.

on fracture-callus formation and mechanical callus quality. It is also debated whether Ca/VitD supplementation supports the fracture-healing process^{19,21–23}. The lack of research is striking given that 70% of fracture patients display vitamin-D deficiency²⁴. Recently, our group investigated fracture healing in a mouse model of hypochlorhydria-induced calcium malabsorption. Notably, bone healing was unaffected, whereas skeletal osteoclast activity was considerably increased post-fracture²³. These results suggest enhanced posttraumatic bone resorption to mobilize calcium from the intact skeleton when the uptake does not meet the requirements for callus mineralization. In agreement with our results, clinical studies observed systemic bone loss following fracture as indicated by a reduction in bone mineral density (BMD) of up to 15% in the intact skeleton^{25,26}. The posttraumatic bone loss may aggravate osteoporosis and explain the significantly increased risk for secondary fractures²⁷. We hypothesize that posttraumatic bone loss might particularly occur under Ca/VitD-deficient conditions, however, to the best of our knowledge, related studies are currently lacking²⁸.

Therefore, we investigated whether chronic dietary Ca/VitD deficiency compromises bone repair and induces posttraumatic bone loss in a mouse model of ovariectomy (OVX)-induced osteoporosis. We also addressed the question whether dietary Ca/VitD supplementation initiated from the time point of fracture augments fracture healing and prevents posttraumatic bone loss.

Results

Effects of dietary calcium and vitamin D on bone turnover in non-fractured ovariectomized mice.

We first characterized the effects of the feeding protocols on bone turnover in non-fractured ovariectomized mice. We used the same experimental setup as in the subsequent fracture healing experiment but did not induce a fracture (Fig. 1). Briefly, following OVX, the control group C received a standard diet whereas groups D and S received a Ca/VitD-deficient diet. After a further 8 weeks, when bone loss was expected to be manifest and when we planned to induce the fracture, group S was switched to a Ca/VitD-supplemented diet (Fig. 1). After another 23 days (planned fracture-healing period), we performed bone and serum analyses. As expected, bone properties were considerably diminished (Fig. 2a) and serum 25(OH)D₃ levels were significantly reduced in Ca/VitD-deficient mice compared to mice with standard diet (Fig. 2b). Serum calcium and phosphate levels did not significantly differ between the groups (Supplemental Table S1), whereas serum PTH levels were significantly increased in deficient mice compared to controls (Fig. 2c). As expected, Ca/VitD deficiency decreased bone mass both in the trabecular and cortical compartments (Table 1). μ CT analysis of lumbar vertebrae and femurs of deficient mice revealed a significantly reduced cortical thickness, bone volume to tissue volume (BV/TV) and trabecular number (Tb.N), whereas trabecular separation was significantly increased compared to controls (Table 1). In comparison to controls, osteoclast surface in lumbar vertebrae was significantly increased, whereas osteoblast number and surface were significantly reduced in deficient mice (Fig. 2e–g). Dynamic histomorphometry revealed significantly reduced bone formation compared to controls (Fig. 2h,k).

Ca/VitD supplementation abolished the osteo-catabolic effects of the deficient diet (Table 1; Fig. 2a). Compared to deficient mice, serum 25(OH)D₃ levels were significantly increased, whereas serum PTH levels were significantly reduced in supplemented mice (Fig. 2b,c). However, serum 25(OH)D₃ levels of supplemented mice were still significantly lower compared to control mice (Fig. 2b). μ CT and histomorphometric analyses revealed a significantly increased BMD, BV/TV and trabecular and cortical thicknesses (Table 1) as well as a reduced number of osteoclasts and an increased osteoblast surface in supplemented mice compared to deficient mice (Fig. 2d,g). In relation to these changes, in supplemented mice the BFR/BS and MS/BS were significantly increased compared to both mice with the deficient and control diet, whereas the MAR was only increased compared to deficient mice (Fig. 2h–k). Further μ CT and histomorphometric parameters did not differ between non-fractured supplemented and control mice (Table 1; Fig. 2), however, we did not assess the amount of presumed bone loss in the skeleton of the mice prior to supplementation when differences between both groups are expected due to the preceding deficiency.

Effects of dietary calcium and vitamin D on fracture healing. We next evaluated the effects of Ca/VitD deficiency on fracture healing in ovariectomized mice. Ten days after osteotomy no significant effects of Ca/VitD deficiency on the callus tissue composition were observed (Fig. 3a,h). However, in the later healing period, Ca/VitD-deficient mice displayed a significantly reduced BMD in the fracture callus compared to control mice (Table 2). BV/TV was not significantly altered (Table 2), whereas in histomorphometry, deficient mice displayed

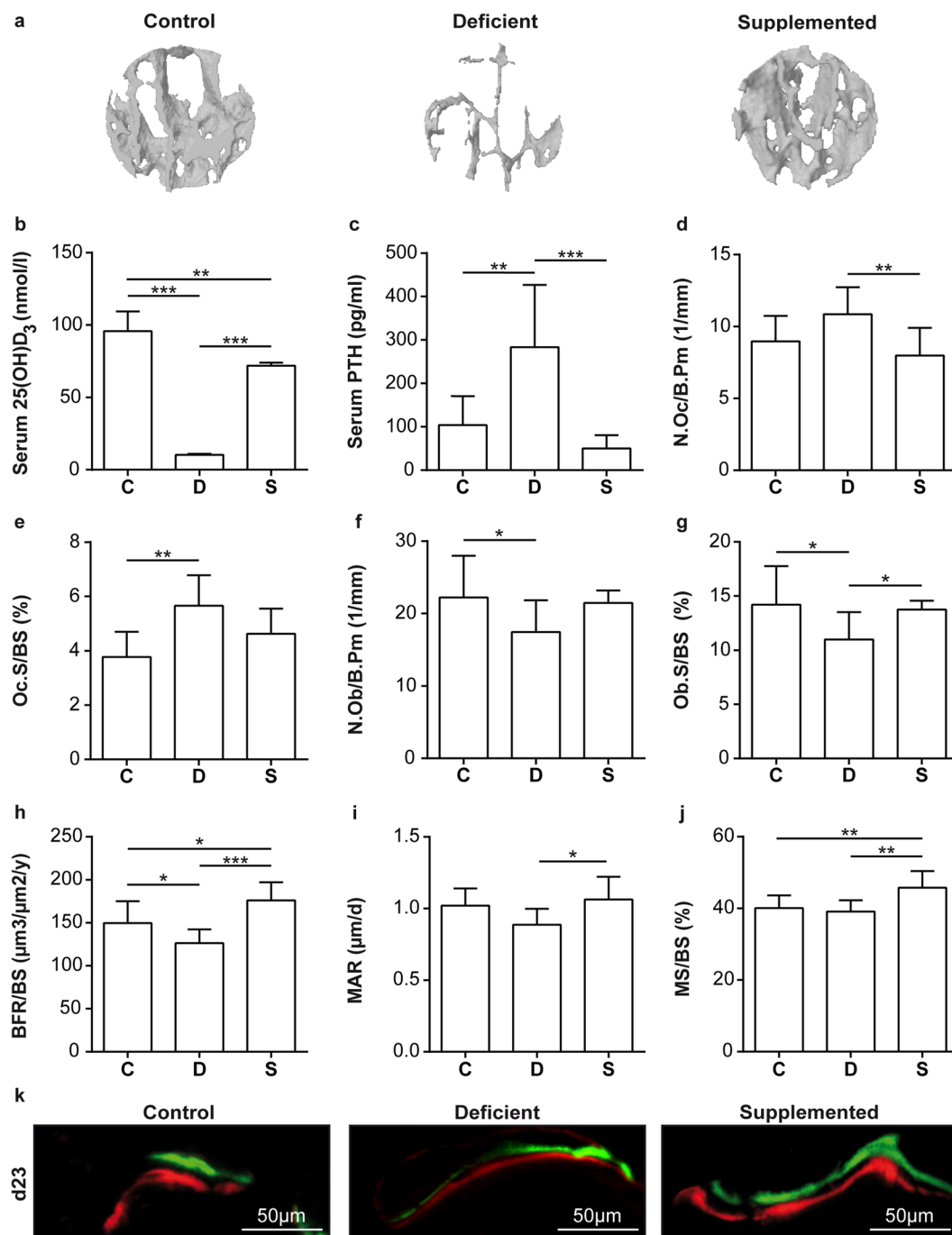


Figure 2. Skeletal examination on day 23 of non-fractured ovariectomized mice fed a control (C), Ca/VitD-deficient (D) or Ca/VitD-supplemented (S) diet. **(a)** Representative 3-dimensional reconstructions (1.3 mm diameter) of trabecular bone in lumbar vertebrae (L2) analyzed by μ CT. **(b)** Serum 25(OH)D₃ ($n = 4/\text{group}$), and **(c)** serum parathyroid hormone (PTH) levels ($n = 5\text{--}6/\text{group}$). **(d)** Number of osteoclasts per bone perimeter (N.Oc./B.Pm), **(e)** osteoclast surface per bone surface (Oc.S/BS), **(f)** number of osteoblasts per bone perimeter (N.Ob/B.Pm), **(g)** osteoblast surface per bone surface (Ob.S/BS), **(h)** bone formation rate per bone surface (BFR/BS), **(i)** mineral apposition rate (MAR), and **(j)** mineralized surface per bone surface (MS/BS) examined in lumbar vertebrae (L2; $n = 8/\text{group}$). **(k)** Representative images of fluorescent calcein green and alizarin red labels of lumbar vertebrae (L2). Data presented as the mean \pm SD. Significant differences between C, D and S evaluated by ANOVA/Fishers LSD *post-hoc*: * $p < 0.05$, ** $p < 0.01$, *** $p < 0.001$.

a significantly reduced amount of bone and a significantly increased amount of fibrous tissue in the newly formed callus (Fig. 3b,h). Furthermore, fewer fractures were completely bridged with bone in the deficient group (Table 2). The flexural rigidity of the fractured femurs did not differ significantly between control and deficient mice (Fig. 3c).

Parameters		C	D	S
		(n = 8)	(n = 8)	(n = 8)
Trabecular bone: lumbar vertebrae (L2)				
Bone mineral density	BMD in HAmg/cm ³	757 ± 29	722 ± 54	791 ± 45 [#]
Bone volume	BV/TV in %	19.4 ± 5.2	12.9 ± 3.6*	19.9 ± 5.8 [#]
Trabecular thickness	Tb.Th in mm	0.057 ± 0.007	0.058 ± 0.007	0.068 ± 0.007*. [#]
Trabecular number	Tb.N in 1/mm	3.4 ± 1.0	2.2 ± 0.7*	2.9 ± 0.6
Trabecular separation	Tb.Sp in mm	0.18 ± 0.04	0.23 ± 0.05*	0.23 ± 0.03*
Cortical bone: femur				
Bone mineral density	BMD in HAmg/cm ³	1266 ± 35	1291 ± 55	1331 ± 74*
Cortical thickness	Ct.Th in mm	0.158 ± 0.002	0.154 ± 0.003*	0.160 ± 0.002*. [#]

Table 1. μ CT analysis of lumbar vertebrae and femurs of non-fractured ovariectomized mice. Data presented as the mean \pm SD. C = control diet; D = Ca/VitD-deficient diet; S = Ca/VitD-supplemented diet. ANOVA/Fishers LSD *post-hoc*; *vs. C $p < 0.05$; [#]vs. D $p < 0.05$.

Fracture callus parameters		C	D	S
		(n = 8)	(n = 9)	(n = 9)
Bone mineral density	BMD in HAmg/cm ³	371 ± 74	303 ± 48*	343 ± 46
Bone volume	BV/TV in %	20 ± 7	18 ± 5	19 ± 6
Tissue volume	TV in mm ³	5.7 ± 2.4	7.1 ± 2.7	7.0 ± 1.8
Healed fractures	in % (total healed)	63 (5 of 8)	56 (5 of 9)	77 (7 of 9)

Table 2. μ CT analysis of the fracture callus of ovariectomized mice on day 23 post-fracture. Data presented as the mean \pm SD. C = control diet; D = Ca/VitD-deficient diet; S = Ca/VitD-supplemented diet. BMD, BV/TV and TV: ANOVA/Fishers LSD *post-hoc*; Healed fractures: Chi-square test; *vs. C $p < 0.05$.

In the fracture calli, the number and surface of osteoclasts were significantly increased, whereas osteoblast parameters were not significantly affected in the deficient group (Fig. 3d–h). Concluding, these data indicate that in deficient mice the bone content was slightly reduced, but the biomechanical properties of the callus were unaffected, suggesting that bone healing was only moderately disturbed in mice with chronic Ca/VitD deficiency.

We also investigated whether the negative effects of the Ca/VitD deficiency on bone repair were abolished when Ca/VitD supplement was provided from the time of fracture. Ca/VitD supplementation provoked no significant effects 10 days after fracture (Fig. 3a,h). In contrast, by day 23, Ca/VitD supplementation slightly increased BMD in the fracture calli, but not significantly (Table 2). However, histomorphometric analysis, which, unlike μ CT, also captures immature, less mineralized bone, revealed a significantly increased bone fraction and a reduced fibrous tissue fraction in the fracture calli of supplemented mice compared to deficient mice (Fig. 3b,h). Consequently, supplemented mice displayed a significantly increased flexural rigidity (Fig. 3c) and the highest percentage of healed fractures (Table 2), which was not statistically different compared to both other groups since the power of the study was insufficient to detect significant differences with the chi-square test. The higher bone fraction in the callus of supplemented mice resulted from reduced osteoclast and increased osteoblast activities (Fig. 3d–h). This was confirmed by a significantly increased mRNA expression of the osteoblast marker ALP in the fracture callus of supplemented mice compared to deficient mice (Fig. 4a) and by reduced serum levels of the bone-resorption marker CTX compared to control mice (Fig. 4b), however the serum levels of the bone-formation marker PINP were unaffected (Fig. 4c). VDR expression was significantly increased in the callus of supplemented mice compared to deficient mice (Fig. 4d), implying enhanced vitamin-D signalling due to Ca/VitD supplementation post-fracture. Concluding, these results suggest that Ca/VitD supplementation initiated at the time of fracture abolished and even overcompensated the negative effects of chronic Ca/VitD deficiency.

We also determined serum FGF23, a major regulator of phosphate and vitamin-D metabolism²⁹. The serum levels of both intact FGF23 (iFGF23) and its inactive C-terminal fragment (cFGF23) were significantly increased in supplemented mice 23 days post-fracture compared to control and deficient mice (Fig. 4e,f), indicating increased systemic FGF23 turnover. However, the ratio of serum iFGF23:cFGF23 levels, representing the biological active FGF23 fraction, did not differ between the groups (Fig. 4g). Confirming this, the protein expression of FGF23 and its main receptor FGFR1 in the fracture callus was not significantly affected by the diet (Fig. 4i). Both FGF23 and FGFR1 were expressed by osteoblasts located on the surface of newly formed bone trabeculae in the callus and by some embedded osteocytes (Fig. 4i). Fracture calli qPCR analysis further confirmed similar FGFR1 and FGF23 mRNA-expression levels in all groups (data not shown). The mRNA expression of Phex, an endopeptidase involved in FGF23 metabolism³⁰, was significantly higher in supplemented mice compared to deficient mice (Fig. 4h), corroborating enhanced FGF23 turnover.

Effects of dietary calcium and vitamin D on posttraumatic bone turnover. We next addressed the question whether dietary calcium and vitamin D influences posttraumatic bone turnover in ovariectomized mice. In deficient mice, PTH serum concentrations continuously increased during fracture healing and were

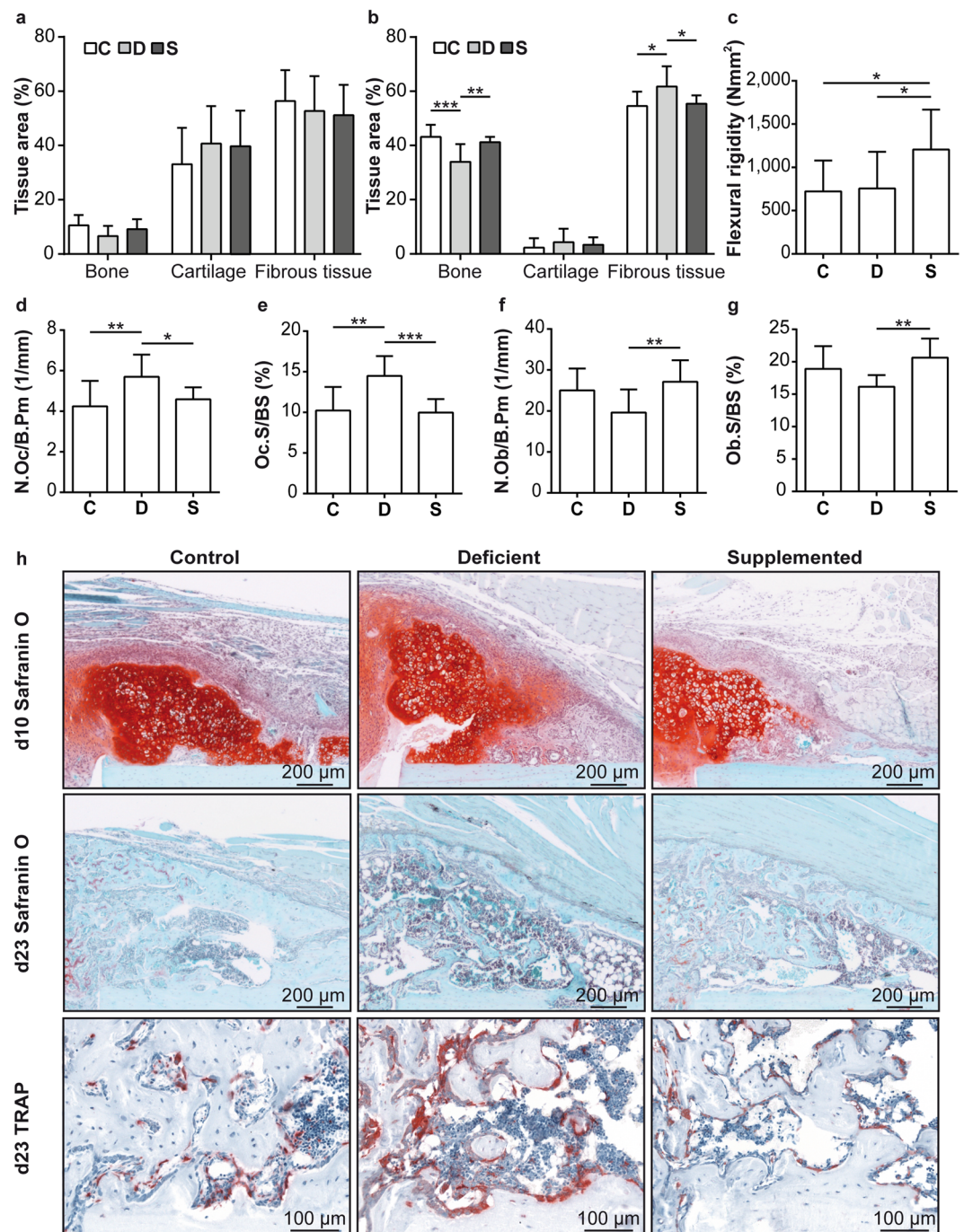


Figure 3. Histomorphometric and biomechanical analysis of fractured femurs in ovariectomized mice fed a control (C), Ca/VitD-deficient (D) or Ca/VitD-supplemented (S) diet. Percentage of bone, cartilage and fibrous tissue in the fracture callus (a) on day 10 (n = 6–8/group) and (b) on day 23 (n = 8/group). (c) Flexural rigidity of fractured femurs on day 23 (n = 8–10/group). (d) Number of osteoclasts per bone perimeter (N.Oc/B.Pm), (e) osteoclast surface per bone surface (Oc.S/BS), (f) number of osteoblasts per bone perimeter (N.Ob/B.Pm) and (g) osteoblast surface per bone surface (Ob.S/BS) in the fracture callus on day 23 (n = 7–9/group). (h) Representative images of the fracture callus stained with Safranin O and tartrate-resistant acid phosphatase (TRAP). Data presented as the mean \pm SD. Significant differences between C, D and S evaluated by ANOVA/Fishers LSD *post-hoc*: * $p < 0.05$, ** $p < 0.01$, *** $p < 0.001$.

significantly higher compared to the control group C on day 23 (Fig. 5a). In addition, PTH serum levels of fractured mice with deficiency were increased compared to the non-fractured mice (PTH in pg/ml: 446 ± 283 Fx vs. 284 ± 173 Non-Fx) on day 23 (Figs 2c and 5a). In agreement with these data, fractured mice of the deficient-diet group exhibited significantly more osteoclasts in the lumbar vertebrae compared to the fractured control group

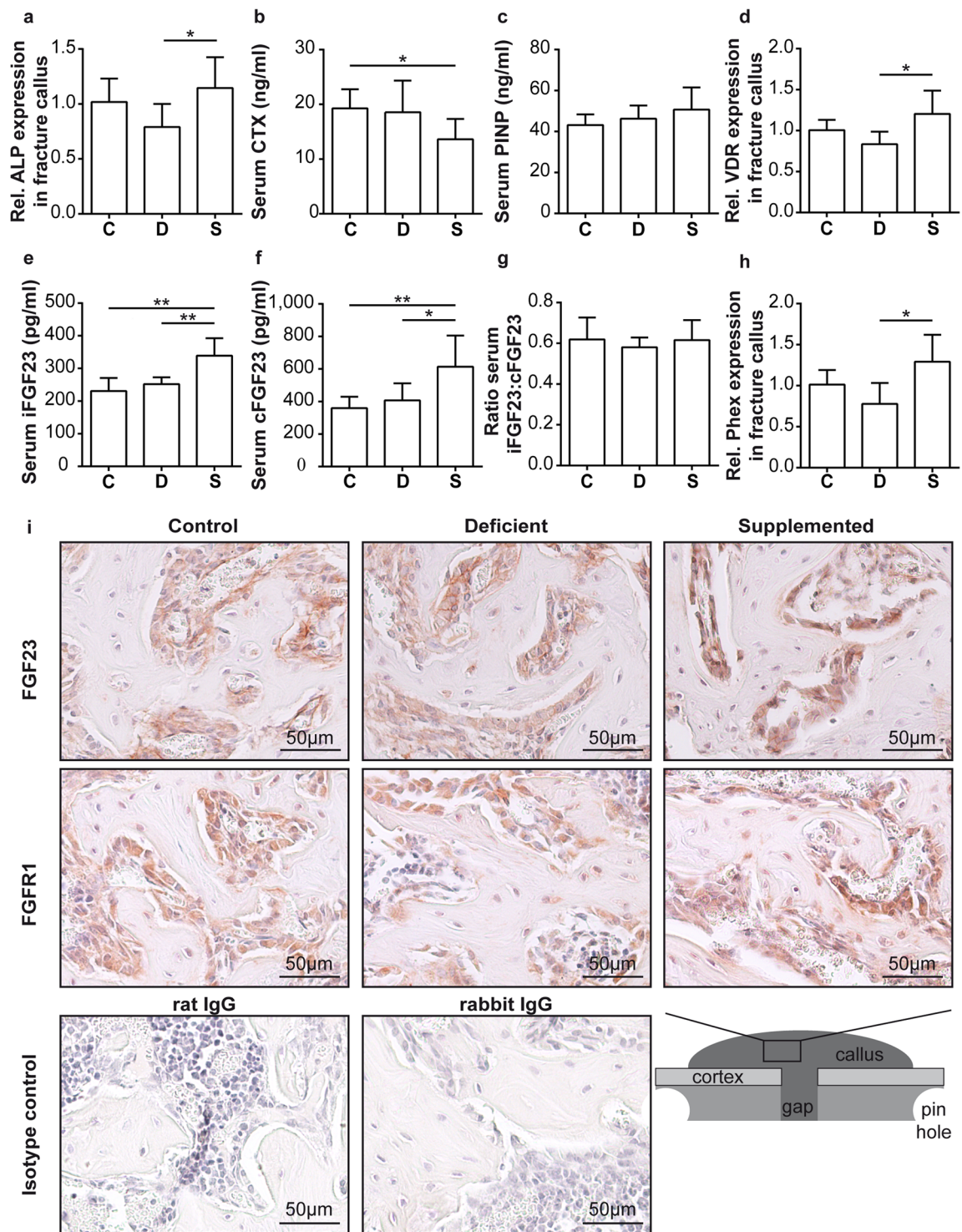


Figure 4. Serum analysis and gene expression and immunohistochemical analyses of the fracture calli of ovariectomized fractured mice fed a control (C), Ca/VitD-deficient (D) or Ca/VitD-supplemented (S) diet on day 23. **(a)** Relative alkaline phosphatase (ALP) gene expression in the fracture calli (n = 4–5/group). **(b)** Serum C-terminal telopeptide of type I collagen (CTX), and **(c)** serum N-terminal propeptide of type I procollagen (PINP) levels (n = 6–7/group). **(d)** Relative vitamin D-receptor (VDR) gene expression in the fracture calli (n = 4–5/group). **(e)** Serum fibroblast intact growth factor 23 (iFGF23) and **(f)** C-terminal FGF23 (cFGF23) levels (n = 5–7/group). **(g)** Ratio of serum iFGF23 to serum cFGF23 levels (n = 5/group). **(h)** Relative phosphate-regulating neutral endopeptidase, X-linked (Phex) gene expression in the fracture calli (n = 4–5/group). **(i)** Representative images of FGF23, fibroblast growth factor receptor 1 (FGFR1) and species-specific isotype control (rat and rabbit IgG) immunostained sections of the fracture calli. For gene expression analyses, β -2-microglobulin was used as the house-keeping gene. Data presented as the mean \pm SD. Significant differences between C, D and S evaluated by ANOVA/Fishers LSD *post-hoc*: * $p < 0.05$, ** $p < 0.01$.

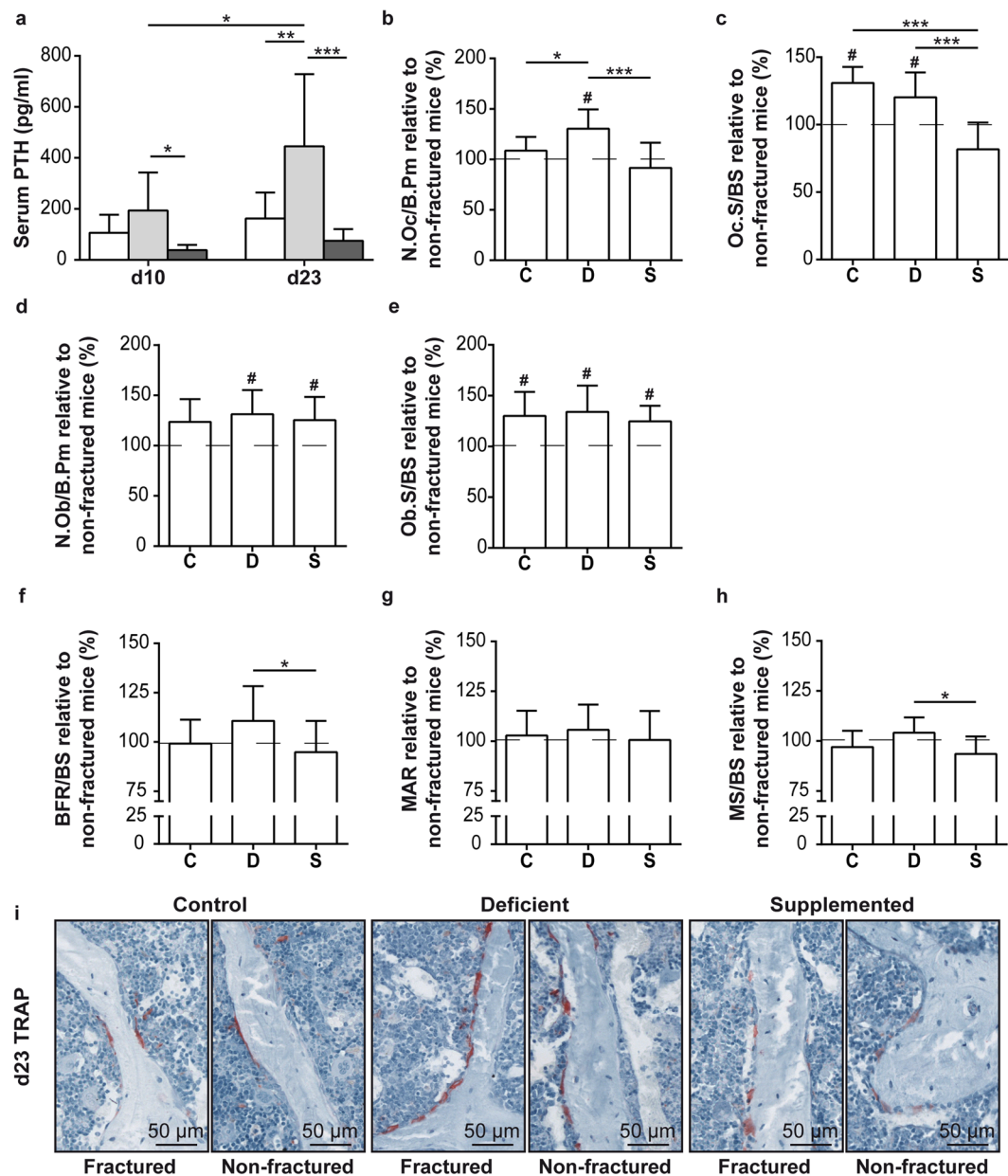


Figure 5. Serum analysis and histomorphometric evaluation of posttraumatic bone turnover in ovariectomized mice fed a control (C), Ca/VitD-deficient (D) or Ca/VitD-supplemented (S) diet. **(a)** Serum parathyroid hormone (PTH) concentrations of fractured mice on day 10 and 23 post-fracture ($n = 6-8/\text{group}$). **(b)** Number of osteoclasts per bone perimeter (N.Oc/B.Pm), **(c)** osteoclast surface per bone surface (Oc.S/BS), **(d)** number of osteoblasts per bone perimeter (N.Ob/B.Pm), **(e)** osteoblast surface per bone surface (Ob.S/BS), **(f)** bone formation rate per bone surface (BFR/BS), **(g)** mineral apposition rate (MAR) and **(h)** mineralized surface per bone surface (MS/BS) of fractured mice relative to non-fractured mice of the same dietary group (dashed line) in percent examined in lumbar vertebrae (L2) on day 23 ($n = 7-9/\text{group}$). **(i)** Representative images of lumbar vertebrae stained with tartrate-resistant acid phosphatase (TRAP) of fractured and non-fractured mice. Data presented as the mean \pm SD. Significant differences between C, D and S: * $p < 0.05$, ** $p < 0.01$, *** $p < 0.001$ evaluated by ANOVA/Fishers LDS *post-hoc*. #Significantly different ($p < 0.05$) from non-fractured mice of the same dietary group (dashed line) evaluated by Student's *t*-test.

and to non-fractured mice with Ca/VitD deficiency (dashed line) (Fig. 5b,i). Osteoclast surface was not significantly different between fractured mice with deficient and standard diets, but was significantly increased compared to the corresponding non-fractured mice (dashed line) (Fig. 5c). Osteoblast number and surface were increased in fractured mice of the deficient and supplemented groups compared to non-fractured mice (dashed line) (Fig. 5d,e). Dynamic histomorphometric analysis revealed a relative increased BFR/BS and MS/BS in deficient mice with fracture compared to supplemented mice with fracture (Fig. 5f,h). However, there were

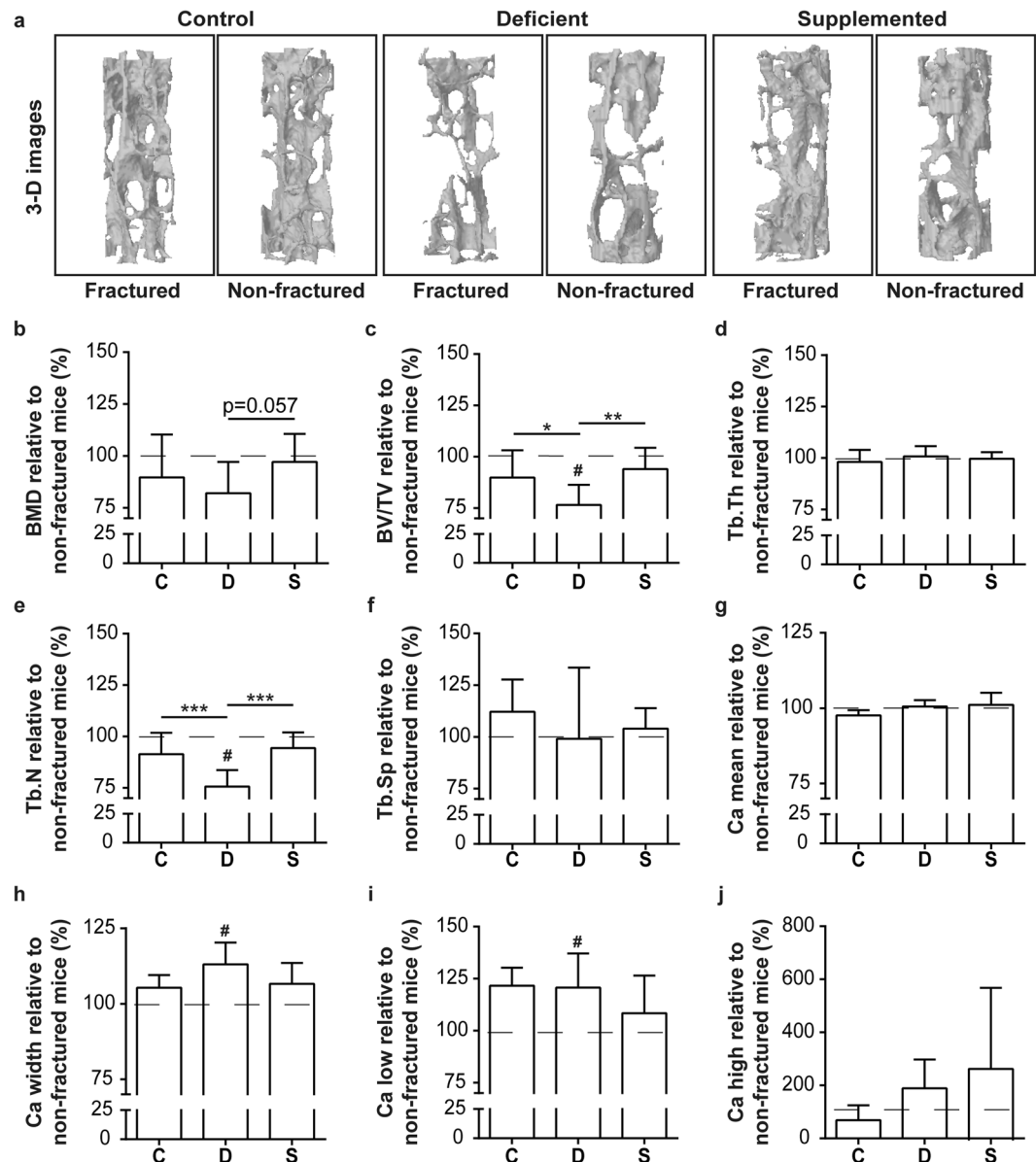


Figure 6. μ CT and quantitative backscattered imaging (qBEI) analysis of posttraumatic bone turnover in ovariectomized mice fed a control (C), Ca/VitD-deficient (D) or Ca/VitD-supplemented (S) diet. (a) Representative 3-dimensional reconstructions (0.8 mm diameter) of trabecular bone in lumbar vertebrae (L2) analyzed by μ CT. (b) Bone mineral density (BMD), (c) bone volume to tissue volume (BV/TV), (d) trabecular thickness (Tb.Th), (e) trabecular number (Tb.N), and (f) trabecular separation (Tb.Sp) of fractured mice relative to non-fractured mice of the same dietary group (dashed line) in percent examined in lumbar vertebrae (L2) on day 23 ($n = 7-9$ /group). (g) Ca mean, (h) Ca width, (i) Ca low and (j) Ca high of fractured mice relative to non-fractured mice of the same dietary group (dashed line) in percent examined in lumbar vertebrae (L2) on day 23 ($n = 5$ /group). Data presented as the mean \pm SD. Significant differences between C, D and S: * $p < 0.05$, ** $p < 0.01$, *** $p < 0.001$ evaluated by ANOVA/Fishers LDS *post-hoc*. #Significantly different ($p < 0.05$) from non-fractured mice of the same dietary group (dashed line) evaluated by Student's *t*-test.

no significant differences in dynamic histomorphometric parameters of fractured mice relative to non-fractured mice (dashed line) (Fig. 5f-h).

μ CT analysis of lumbar vertebrae identified a significantly reduced BV/TV and Tb.N of fractured deficient mice relative to non-fractured mice with deficiency (dashed line) and compared to fractured control mice (Fig. 6a,c,e), thus indicating increased posttraumatic bone loss under Ca/VitD deficient conditions. In addition, qBEI analysis of lumbar vertebrae revealed a significantly increased Ca low and a higher heterogeneity (Ca width) in fractured deficient mice relative to deficient mice without fracture (Fig. 6h,i), suggesting a higher fraction of very low mineralized bone after fracture. Further qBEI parameters did not differ between the dietary groups and between fractured and non-fractured mice (Fig. 6g-j). Taken together, these data suggest a pronounced

posttraumatic bone resorption under Ca/VitD deficiency induced by increased PTH serum levels leading to a posttraumatic reduction in bone mass and mineral.

Ca/VitD supplementation abolished the posttraumatic PTH increase (Fig. 5a). In agreement with these findings, the osteoclast activity in the lumbar vertebral bodies of fractured mice with supplementation was significantly reduced compared to fractured mice with the deficient diet (Fig. 5b,c,i). In addition, BMD was increased by trend ($p = 0.057$) and BV/TV and Tb.N were significantly increased after Ca/VitD supplementation compared to deficient mice (Fig. 6a–c,e). Furthermore, Ca low and Ca width did not differ between fractured supplemented mice and supplemented mice without fracture (Fig. 6h,i). In addition, Ca/VitD supplementation slightly but not significantly reduced Ca width and Ca low, as well as increased Ca high compared to fractured deficient mice (Fig. 6h–j). These data indicate that Ca/VitD supplementation post-fracture ameliorated posttraumatic bone resorption and bone loss.

Discussion

In this study we investigated the role of calcium and vitamin-D in fracture healing and posttraumatic bone turnover in a mouse model of OVX-induced osteoporosis. Fracture healing was almost not affected in mice with chronic dietary Ca/VitD deficiency. In contrast, these mice did display significantly increased serum PTH levels as well as increased osteoclast activity and reduced bone mass and mineralization in the intact skeleton post-fracture, indicating increased calcium mobilization from the intact skeleton during bone healing. Ca/VitD supplementation initiated at time of fracture improved healing and abolished posttraumatic bone resorption. Therefore, our study demonstrates the importance of a sufficient calcium and vitamin-D supply during fracture healing to provide sufficient dietary calcium for callus mineralization and to prevent posttraumatic bone loss, and is, thus, clinically highly relevant.

To mimic chronic Ca/VitD deficiency in postmenopausal females, we used ovariectomized mice that received a diet without Ca/VitD. In agreement with the limited earlier studies in rodents^{31–33}, we demonstrated that in non-fractured mice Ca/VitD deficiency significantly increased systemic PTH levels and bone resorption and decreased bone formation, resulting in a reduced cortical and trabecular bone mass. Ca/VitD supplementation for 3 weeks almost completely abolished the catabolic effects of the 8 weeks of deficiency, in agreement with experimental studies in rats and mice^{34–37}. Additionally, several clinical trials of Ca/VitD supplementation in aged, postmenopausal females described increased BMD and a reduced fracture risk^{38,39}. Therefore, our mouse model mimics clinical Ca/VitD deficiency in postmenopausal females, thus making it suitable to study fracture healing and posttraumatic bone turnover under these conditions.

Because calcium is essential for callus mineralization during bone regeneration^{16,17}, we investigated whether Ca/VitD deficiency influenced bone repair. The Ca/VitD-deficient mice displayed moderately impaired fracture healing as indicated by a reduced bone fraction and increased osteoclast numbers in the fracture callus. The high systemic PTH levels in deficient mice may be responsible for the significantly increased osteoclast activity in the callus. Regarding the effects of Ca/VitD deficiency on bone healing, there are only a limited number of rat studies, some published much earlier, which reported contradictory effects on callus mineralization and biomechanical bone properties^{18–20,40}. In agreement with our results, patients with impaired healing and non-unions frequently displayed lower vitamin-D serum levels compared to patients with uneventful healing^{41–43}. Importantly, we demonstrated that Ca/VitD supplementation abolished the negative effects of the previously deficient diet, as demonstrated by an increased fracture-callus bone fraction. Supporting this, osteoblast numbers and ALP in the callus were increased, whereas osteoclast numbers and serum CTX were diminished, due to reduced serum PTH levels in supplemented mice. Furthermore, the bending stiffness of the healed femurs was considerably increased due to a higher percentage of bony bridged fracture gaps, further confirming improved fracture healing following Ca/VitD supplementation. Again, experimental studies in rodents reported contradictory results regarding the effects of Ca/VitD administration on fracture healing^{21–23}, which may result from the widely varying experimental conditions. However, our results are in agreement with clinical data. In a prospective, randomized study, postmenopausal females who received Ca/VitD supplementation displayed higher BMD in the fracture region after 6 weeks compared to patients receiving placebo⁴⁴.

It is hypothesized that vitamin D exerts its positive effects on bone regeneration mainly indirectly through its endocrine action on calcium homeostasis², thus increasing the calcium supply for fracture callus mineralization. However, direct vitamin-D effects on bone are also widely discussed, because osteoblasts express the VDR and its expression on these cells is directly regulated by biologically active $1,25(\text{OH})_2\text{D}_3$ ^{45,46}. Several *in-vitro* studies demonstrated that $1,25(\text{OH})_2\text{D}_3$ binding to the VDR enhanced osteoblast differentiation and mineralization, which is often indicated by the increased activity of the osteoblast differentiation marker ALP^{47,48}. The present study demonstrated increased expression of VDR and ALP in the fracture callus of supplemented mice. Based on these results, we propose that enhanced $1,25(\text{OH})_2\text{D}_3/\text{VDR}$ signalling locally in the fracture callus may also contribute to Ca/VitD-treatment induced fracture-healing improvement. However, further studies need to investigate the exact mechanisms responsible for the changes resulting from the dietary treatments.

We also investigated FGF23 because it is a regulator of mineral and vitamin D metabolism and was proposed to be important for efficient bone healing⁴⁹. In supplemented mice, both intact FGF23 (iFGF23) and the inactive proteolytic C-terminal fragment (cFGF23) serum levels were significantly increased, indicating enhanced FGF23 turnover. However, the iFGF23:cFGF23 ratio was unaltered, possibly indicating unchanged biologically active FGF23. Supporting this, FGF23 and FGFR1 expression in the fracture callus was not influenced by supplementation, suggesting that local FGF23 signalling was unaffected. The increased endopeptidase Phex mRNA expression in the fracture callus, which is thought to be involved in FGF23 cleavage³⁰, supports enhanced FGF23 turnover in supplemented mice. However, further investigations are needed to clarify these observations.

We recently demonstrated that while fracture healing was unaffected in mice with intestinal calcium malabsorption, osteoclast activity in the intact skeleton was significantly increased, suggesting increased posttraumatic

bone resorption²³. In the present study, we confirmed these results. Ca/VitD-deficient mice similarly exhibited increased PTH serum levels post-fracture and enhanced osteoclast activity in the intact skeleton compared to non-fractured mice. In addition, PTH serum levels were higher in fractured mice in comparison to non-fractured mice with deficiency, thus corroborating fracture-induced changes in PTH serum levels. In agreement with our findings, increased post-fracture PTH serum levels were observed in several clinical studies^{50–52}. Notably, elevated serum PTH could still be detected a year post-fracture in postmenopausal females⁵². Several clinical studies observed systemic bone loss after fracture^{25, 26, 53}, thus possibly contributing to the considerably increased risk for secondary fractures^{27, 54}. One such study demonstrated that reduced bone mass after fracture significantly correlated with a reduced dietary calcium intake as well as with low vitamin-D serum levels⁵³, indicating that Ca/VitD deficiency may aggravate posttraumatic bone loss. In agreement with these clinical findings and our previous data, we similarly detected altered bone mineralization in the intact skeleton post-fracture. Deficient mice with fracture exhibited a reduced bone mass and a higher percentage of less mineralized bone areas compared to non-fractured mice with deficiency, thus indicating posttraumatic bone loss. This suggests that Ca/VitD-deficient mice release calcium from their intact skeleton to provide sufficient calcium for callus mineralization. The increased posttraumatic calcium mobilization may explain why healing was only marginally compromised by Ca/VitD deficiency, however, at the clear expense of the intact skeleton. Ca/VitD supplementation after fracture prevented posttraumatic bone loss by reducing serum PTH levels and osteoclastic bone resorption. Supporting this, a clinical study reported decreased PTH serum levels in elderly patients treated post-fracture with Ca/VitD, whereas PTH levels were elevated in the placebo group⁵¹. These findings and our results corroborate the clinical therapeutic requirement for Ca/VitD supplementation post-fracture.

In conclusion, our results indicate that under Ca/VitD deficiency, calcium is increasingly mobilized from the intact skeleton to allow efficient fracture healing. The resulting posttraumatic bone loss may contribute to the 3-fold increased risk of secondary fractures in osteoporotic patients, which are associated with a dramatic increase in patient morbidity and mortality and a reduction in the quality of life⁵⁵. Ca/VitD supplementation initiated at the time of fracture augmented bone repair and prevented posttraumatic bone loss, demonstrating the clinical need for Ca/VitD treatment to reduce fracture-healing complications in osteoporotic patients and to prevent fracture-induced bone loss.

Materials and Methods

Study design. The animal experiment was approved by the Local Ethical Committee (No. 1184, Regierungspräsidium Tübingen, Germany) and was in compliance with international recommendations for the care and use of laboratory animals (ARRIVE guidelines and EU Directive 2010/63/EU for animal experiments). Female C57BL/6J mice were purchased from JanvierLabs (Saint-Berthevi, France). Mice were given *ad libitum* access to water and food, receiving a standard mouse feed (R/M-H, V1535–300, Ssniff Spezialdiäten, Soest, Germany). When aged 16 weeks, the feed was switched to a phytoestrogen-reduced diet (R/M-H, V1554–300, Ssniff). OVX was performed when aged 18 weeks, and the mice were randomly assigned to three groups (Fig. 1). The control group C was continuously fed with the phytoestrogen-reduced diet after OVX, whereas groups D and S received a Ca/VitD-deficient diet (S8276-E710, 0.25% calcium, 0 IU/kg vitamin D, Ssniff) in order to study the proof-of-principle of a severe Ca/VitD deficiency on bone repair and posttraumatic bone turnover, although a milder insufficiency would be more reflective of the majority of osteoporotic patients. All mice received a femur osteotomy 8 weeks after OVX. Group S was transferred to a Ca/VitD-supplemented diet (S8276-E712, 2.0% calcium, 2000 IU/kg vitamin D, Ssniff) immediately after surgery. We included additional control groups, which were treated as described above but received no osteotomy (non-fractured mice; Fig. 1). Mice were euthanized on days 10 and 23 ($n = 5–10$), and fracture healing and posttraumatic bone turnover were evaluated.

Surgery. OVX and femur osteotomy were performed under general anesthesia using 2% isoflurane (Florene, Abbott, Wiesbaden, Germany). For analgesia, mice received 25 mg/ml tramadol hydrochloride (Tramal®, Gruenenthal, Aachen, Germany) in the drinking water, starting one day preoperatively until three days postoperatively. Before surgery, mice received one subcutaneous injection of the antibiotics clindamycin-2-dihydrogenphosphate (45 mg/kg, Ratiopharm, Ulm, Germany). Mice were bilaterally ovariectomized by ligation of the oviduct and removal of the ovary. Femur osteotomy was performed as described previously²³. Briefly, at the midshaft of the right femur an osteotomy gap (0.4 mm) was created and stabilized using an external fixator (axial stiffness 3 N/mm, RISystems, Davos, Switzerland). The mice were injected after 10 days with calcein green (0.03 g/ml, Sigma-Aldrich, St. Louis, USA) and after 15 days with alizarin red (0.045 g/ml, Sigma-Aldrich) for dynamic bone histomorphometry.

Serum analysis. Blood samples were obtained on the day of euthanasia by heart puncture. Serum 25-hydroxy vitamin D₃ (25(OH)D₃), the bone-resorption marker C-terminal telopeptide of type I collagen (CTX) and the bone-formation marker N-terminal propeptide of type I procollagen (PINP) were determined using commercially available enzyme-immunoassay (EIA) kits (25-hydroxy vitamin D EIA, AC57F1; RatLaps™ (CTX-I) EIA, AC-06F1; Rat/Mouse PINP EIA, AC-33F1; all Immunodiagnostic Systems, Frankfurt, Germany). Parathyroid hormone (PTH) and fibroblast growth factor 23 (FGF23; intact and C-terminal) serum levels were determined using enzyme-linked immunosorbent assay (ELISA) kits (Mouse PTH 1-84 ELISA Kit 60-2305; Mouse/Rat FGF-23 (C-Term) ELISA Kit 60-6300; Mouse/Rat FGF-23 (Intact) ELISA Kit 60-6800; all Immotopics Inc., San Clemente, USA). Colorimetric kits were used to determine serum calcium and phosphate levels (QuantiChrom™ Calcium Assay Kit, DICA-500; QuantiChrom™ Phosphate Assay Kit, DIPA-500, both BioAssay, Hayward, USA).

Biomechanical testing. To evaluate biomechanical competence, femurs explanted at day 23 were tested by a non-destructive, three-point-bending test using a material-testing machine (1454, Zwick, Ulm, Germany)²³.

Briefly, after fixator removal, an axial load with a maximum load of 4-N was applied at the midshaft of the femurs and the load and deflection were recorded. Flexural rigidity of the bones was calculated using the linear elastic part of the load-deflection curve.

Micro-computed tomography (μ CT) analysis. On day 23, femurs and lumbar vertebrae were imaged using a μ CT scanning device (Skyscan 1172, Kontich, Belgium) operating at a resolution of 8 μ m and a voltage of 50 kV and 200 μ A. Calibration (hydroxyapatite (HA) phantoms: 250 and 750 mg/cm³) and global thresholding (callus and cortical bone: 641.9 mg HA/cm³; trabecular bone: 394.8 mg HA/cm³) were conducted and intact femurs, lumbar vertebrae and the fracture calli were evaluated as described previously⁵⁶. Common standard parameters of the American Society for Bone and Mineral Research (ASBMR) were determined using Skyscan software (NRecon, DataViewer, CTAn)⁵⁷. To evaluate bony bridging of the fracture gap, the number of bridged cortices per callus was evaluated in two perpendicular planes using μ CT images. When ≥ 3 bridged cortices per callus were observed, the fracture was considered as 'successfully healed'.

Histomorphometry and immunohistochemistry. Femurs and lumbar vertebrae explanted on days 10 and 23 were embedded in methyl methacrylate or paraffin⁵⁶. For histomorphometric analysis of the fracture callus, the specimens were stained using Safranin O and the relative amounts of bone, cartilage and fibrous tissue in the whole callus between the two inner pinholes were determined using image-analysis software (Leica MMAF 1.4.0 Imaging System, Leica, Wetzlar, Germany). Cellular parameters were evaluated in femurs and lumbar vertebrae according to the ASBMR guidelines at day 23 after staining with tartrate-resistant acid phosphatase or toluidine blue⁵⁸. Osteoblasts and osteoclasts were counted in a 1.8 \times 0.9-mm region in the middle of the fracture callus and a 0.6 \times 0.6-mm region centered in the second lumbar vertebral body using the image analysis software Osteomeasure[®] (OsteoMetrics, Decatur, USA). The mineral-apposition rate (MAR), bone-formation rate per bone surface (BFR/BS) and mineralized surface per bone surface (MS/BS) were determined in the second lumbar vertebral body (d23; 0.6 \times 0.6 mm centered region) using Osteomeasure[®] image analysis (OsteoMetrics).

Paraffin-embedded sections of fractured femurs (d23) were immunohistochemically stained for FGF23 and fibroblast growth factor receptor 1 (FGFR1) using the following antibodies and dilutions: rat anti-mouse FGF23, 1:100 (MAB26291, R&D systems Inc., Minneapolis, USA), rabbit anti-mouse FGFR1/CD331, 1:50 (PA5-25979, Invitrogen, Thermo Fisher Scientific, Waltham, USA), goat anti-rabbit immunoglobulin G (IgG) (H + L) biotin-conjugated, 1:100 (B2770, Invitrogen), and goat anti-rat IgG (H + L) biotin-conjugated, 1:100 (A10517, Invitrogen). Species-specific IgGs were used for isotype controls. Signal amplification was performed using the avidin-biotin complex (Vector, Burlingame, USA). Substrate was detected using NovaRed (Vector) and the sections were counterstained using hematoxylin (Waldeck, Münster, Germany).

Quantitative backscattered electron imaging (qBEI) analysis. To determine mineral content and distribution in lumbar vertebrae, qBEI was performed as described previously^{23, 59}. Briefly, segments of lumbar vertebrae embedded in methyl methacrylate (d23) were polished, coated with carbon and analyzed using a scanning electron microscope (LEO 435 VP, LEO Electron Microscopy Ltd., Cambridge, England) operating at 20 kV and 665 pA at a constant working distance (BSE Detector, Type 202, K.E. Developments Ltd., Cambridge, England) with a 2.29- μ m pixel size. For calibration, an aluminium carbon standard was used⁶⁰. From the generated grey value images we calculated the mean calcium content (Ca mean wt%), the heterogeneity of mineralization (Ca width wt%), the fraction of highly (Ca high %) and poorly (Ca low %) mineralized bone areas of the lumbar vertebrae.

Gene-expression analysis of the fracture callus. On day 23, the fracture calli were harvested and stored in RNAlater[™] (Sigma-Aldrich) at 4 °C. Following RNAlater[™] removal, the fracture callus was snap-frozen in liquid nitrogen and pulverized in a vibration mill at 30 Hz for 1.5 minutes. Total RNA was isolated using the TRIzol Plus RNA Purification Kit (Ambion, Thermo Fisher Scientific, Waltham, USA) according to the manufacturer's instructions plus an additional DNA-digestion step using the RNase-Free DNase Set (50) (Qiagen, Hilden, Germany). In total, 1 μ g of isolated RNA was transcribed into cDNA using the Omniscript RT kit (Qiagen). Quantitative polymerase chain reaction (qPCR) was performed using the Brilliant Sybr Green qPCR Master Mix Kit (Stratagene, Amsterdam, Netherlands) according to the manufacturer's protocol. Alkaline phosphatase (ALP, F: 5'-GCTGATCATTCCCACGTTT-3' and R: 5'-GAGCCAGACCAAAGATGGAG-3'), vitamin D-receptor (VDR, F: 5'-GGGCTTCCACTTCAACGCTA-3' and R: 5'-CATGCTCCGCCTGAAGAAAC-3'), phosphate-regulating neutral endopeptidase, X-linked (Phex, F: 5'-TTCCCCAGTTTGACTGGCTG-3' and R: 5'-TCTCCGAGGACCAATGTCT-3'), FGF23 (F: 5'-ACAGGAGCCATGACTCGAAG-3' and R: 5'-GCAATTCTCTGGGCTGAAGT-3'), and FGFR1 (F: 5'-TGACGACGACGATGACTCCT-3' and R: 5'-AGCTACAGGCCTACGGTTTG-3') expression were normalized to the housekeeping gene β -2-microglobulin (F: 5'-ATACGCCTGCAGAGTTAAGCA-3' and R: 5'-TCACATGTCTCGATCCAGT-3'). The normalized relative amounts of targets were then compared to the target signals of the control group using the delta-delta CT method with PCR-efficiency correction using LinRegPCR software (Heart Failure Research Center, Academic Medical Center, Amsterdam, Netherlands) as described previously⁶¹.

Statistical Analysis. Results are presented as the mean \pm standard deviation (SD). Statistical analysis was performed using GraphPad Prism 6 software (GraphPad Software, Inc., La Jolla, USA). Normal distribution of data was tested by Shapiro-Wilk normality test. Data were analysed for significance either by one-way analysis of variance (ANOVA) and Fishers LSD *post-hoc* when three groups were compared to each other or by Student's *t*-test when two groups were compared. For the comparison of fractured and non-fracture mice, the values of the fractured mice were indicated relative to the values of the non-fractured mice of the same dietary group in

percent (%). Data of healed fractures were analysed by chi-square test. The level of significance was set $p < 0.05$. The number of samples for each experiment is indicated in the figure legends and tables. Sample size was calculated based on the main outcome parameter flexural rigidity of the fractured femur (power: 80%, $\alpha = 0.05$) obtained from previous studies²³.

Data availability statement. All relevant data are included within the manuscript. Data can be provided upon request.

References

- Rachner, T. D., Khosla, S. & Hofbauer, L. C. Osteoporosis: now and the future. *Lancet*. **377**, 1276–1287 (2011).
- Carmeliet, G., Dermauw, V. & Bouillon, R. Vitamin D signaling in calcium and bone homeostasis: a delicate balance. *Best practice & research. Clinical endocrinology & metabolism*. **29**, 621–631 (2015).
- Lips, P. & van Schoor, N. M. The effect of vitamin D on bone and osteoporosis. *Best practice & research. Clinical endocrinology & metabolism*. **25**, 585–591 (2011).
- Priemel, M. *et al.* Bone mineralization defects and vitamin D deficiency: histomorphometric analysis of iliac crest bone biopsies and circulating 25-hydroxyvitamin D in 675 patients. *J Bone Miner Res*. **25**, 305–312 (2010).
- Hossein-Nezhad, A. & Holick, M. F. Vitamin D for health: a global perspective. *Mayo Clin Proc*. **88**, 720–755 (2013).
- Ireland, P. & Fordtran, J. S. Effect of dietary calcium and age on jejunal calcium absorption in humans studied by intestinal perfusion. *J Clin Invest*. **52**, 2672–2681 (1973).
- MacLaughlin, J. & Holick, M. F. Aging decreases the capacity of human skin to produce vitamin D₃. *J Clin Invest*. **76**, 1536–1538 (1985).
- Wakimoto, P. & Block, G. Dietary intake, dietary patterns, and changes with age: an epidemiological perspective. *J Gerontol A Biol Sci Med Sci*. **56 Spec No 2**, 65–80 (2001).
- Cosman, F. *et al.* Clinician's Guide to Prevention and Treatment of Osteoporosis. *Osteoporos Int*. **25**, 2359–2381 (2014).
- Bellantionio, S., Fortinsky, R. & Prestwood, K. How well are community-living women treated for osteoporosis after hip fracture? *J Am Geriatr Soc*. **49**, 1197–1204 (2001).
- Follin, S. L., Black, J. N. & McDermott, M. T. Lack of diagnosis and treatment of osteoporosis in men and women after hip fracture. *Pharmacotherapy*. **23**, 190–198 (2003).
- Kuchuk, N. O., van Schoor, N. M., Pluijm, S. M., Chines, A. & Lips, P. Vitamin D status, parathyroid function, bone turnover, and BMD in postmenopausal women with osteoporosis: global perspective. *J Bone Miner Res*. **24**, 693–701 (2009).
- Gennari, C. Calcium and vitamin D nutrition and bone disease of the elderly. *Public Health Nutr*. **4**, 547–559 (2001).
- Nikolaou, V. S., Efsthopoulos, N., Kontakis, G., Kanakaris, N. K. & Giannoudis, P. V. The influence of osteoporosis in femoral fracture healing time. *Injury*. **40**, 663–668 (2009).
- Giannoudis, P., Tzioupis, C., Almkali, T. & Buckley, R. Fracture healing in osteoporotic fractures: is it really different? A basic science perspective. *Injury*. **38**(Suppl 1), S90–99 (2007).
- Bauer, G. C. Rate of bone salt formation in a healing fracture determined in rats by means of radiocalcium. *Acta orthopaedica Scandinavica*. **23**, 169–191 (1954).
- Lemaire, R. G. Calcium metabolism in fracture healing. An experimental kinetic study in rats, using Ca⁴⁵. *The Journal of bone and joint surgery. American volume*. **48**, 1156–1170 (1966).
- Doepfner, W. Consequences of calcium and/or phosphorus deficient diets on various parameters of callus formation and on growth rate in young rats. *British journal of pharmacology*. **39**, 188P–189P (1970).
- Einhorn, T. A., Bonnarens, F. & Burstein, A. H. The contributions of dietary protein and mineral to the healing of experimental fractures. A biomechanical study. *The Journal of bone and joint surgery. American volume*. **68**, 1389–1395 (1986).
- Melhus, G. *et al.* Experimental osteoporosis induced by ovariectomy and vitamin D deficiency does not markedly affect fracture healing in rats. *Acta Orthop*. **78**, 393–403 (2007).
- Fu, L., Tang, T., Miao, Y., Hao, Y. & Dai, K. Effect of 1,25-dihydroxy vitamin D₃ on fracture healing and bone remodeling in ovariectomized rat femora. *Bone*. **44**, 893–898 (2009).
- Shuid, A. N. *et al.* Effects of calcium supplements on fracture healing in a rat osteoporotic model. *J Orthop Res*. **28**, 1651–1656 (2010).
- Haffner-Luntzer, M. *et al.* Hypochlorhydria-induced calcium malabsorption does not affect fracture healing but increases post-traumatic bone loss in the intact skeleton. *J Orthop Res*. **34**, 1914–1921 (2016).
- Sprague, S. *et al.* What Is the Role of Vitamin D Supplementation in Acute Fracture Patients? A Systematic Review and Meta-Analysis of the Prevalence of Hypovitaminosis D and Supplementation Efficacy. *J Orthop Trauma*. **30**, 53–63 (2016).
- Karlsson, M. K. *et al.* Bone loss following tibial osteotomy: a model for evaluating post-traumatic osteopenia. *Osteoporos Int*. **11**, 261–264 (2000).
- Fox, K. M. *et al.* Loss of bone density and lean body mass after hip fracture. *Osteoporos Int*. **11**, 31–35 (2000).
- Ahmed, L. A. *et al.* Progressively increasing fracture risk with advancing age after initial incident fragility fracture: the Tromso study. *J Bone Miner Res*. **28**, 2214–2221 (2013).
- Gorter, E. A., Hamdy, N. A., Appelman-Dijkstra, N. M. & Schipper, I. B. The role of vitamin D in human fracture healing: a systematic review of the literature. *Bone*. **64**, 288–297 (2014).
- DiGirolamo, D. J., Clemens, T. L. & Kousteni, S. The skeleton as an endocrine organ. *Nat Rev Rheumatol*. **8**, 674–683 (2012).
- Beck, L. *et al.* Pex/PEX tissue distribution and evidence for a deletion in the 3' region of the Pex gene in X-linked hypophosphatemic mice. *J Clin Invest*. **99**, 1200–1209 (1997).
- Jiang, Y., Zhao, J., Genant, H. K., Dequeker, J. & Geusens, P. Long-term changes in bone mineral and biomechanical properties of vertebrae and femur in aging, dietary calcium restricted, and/or estrogen-deprived/-replaced rats. *J Bone Miner Res*. **12**, 820–831 (1997).
- Han, S. M., Szarzanowicz, T. E. & Ziv, I. Effect of ovariectomy and calcium deficiency on the ultrasound velocity, mineral density and strength in the rat femur. *Clin Biomech (Bristol, Avon)*. **13**, 480–484 (1998).
- Kaastad, T. S. *et al.* Vitamin D deficiency and ovariectomy reduced the strength of the femoral neck in rats. *Calcified tissue international*. **69**, 102–108 (2001).
- Lee, A. M. *et al.* Adequate dietary vitamin D and calcium are both required to reduce bone turnover and increased bone mineral volume. *The Journal of steroid biochemistry and molecular biology*. **144 Pt A**, 159–162 (2014).
- Agata, U. *et al.* The Impact of Different Amounts of Calcium Intake on Bone Mass and Arterial Calcification in Ovariectomized Rats. *J Nutr Sci Vitaminol (Tokyo)*. **61**, 391–399 (2015).
- Amling, M. *et al.* Rescue of the skeletal phenotype of vitamin D receptor-ablated mice in the setting of normal mineral ion homeostasis: formal histomorphometric and biomechanical analyses. *Endocrinology*. **140**, 4982–4987 (1999).
- Li, Y. C. *et al.* Normalization of mineral ion homeostasis by dietary means prevents hyperparathyroidism, rickets, and osteomalacia, but not alopecia in vitamin D receptor-ablated mice. *Endocrinology*. **139**, 4391–4396 (1998).

38. Prentice, R. L. *et al.* Health risks and benefits from calcium and vitamin D supplementation: Women's Health Initiative clinical trial and cohort study. *Osteoporos Int.* **24**, 567–580 (2013).
39. Tang, B. M., Eslick, G. D., Nowson, C., Smith, C. & Bensoussan, A. Use of calcium or calcium in combination with vitamin D supplementation to prevent fractures and bone loss in people aged 50 years and older: a meta-analysis. *Lancet.* **370**, 657–666 (2007).
40. Lindgren, J. U., Narechania, R. G., McBeath, A. A., Lange, T. A. & DeLuca, H. F. Effects of 1,24 dihydroxyvitamin D3 and calcitonin on fracture healing in adult rats. *Clinical orthopaedics and related research*, 304–308 (1981).
41. Warner, S. J., Garner, M. R., Nguyen, J. T. & Lorich, D. G. Perioperative vitamin D levels correlate with clinical outcomes after ankle fracture fixation. *Arch Orthop Trauma Surg.* **136**, 339–344 (2016).
42. Di Monaco, M., Vallerio, E., Di Monaco, R., Tappero, R. & Cavanna, A. 25-hydroxyvitamin D, parathyroid hormone, and functional recovery after hip fracture in elderly patients. *J Bone Miner Metab.* **24**, 42–47 (2006).
43. Pourfeizi, H. H., Tabriz, A., Elmi, A. & Aslani, H. Prevalence of vitamin D deficiency and secondary hyperparathyroidism in nonunion of traumatic fractures. *Acta Med Iran.* **51**, 705–710 (2013).
44. Doetsch, A. M. *et al.* The effect of calcium and vitamin D3 supplementation on the healing of the proximal humerus fracture: a randomized placebo-controlled study. *Calcified tissue international.* **75**, 183–188 (2004).
45. van Leeuwen, J. P., Pols, H. A., Schilte, J. P., Visser, T. J. & Birkenhager, J. C. Modulation by epidermal growth factor of the basal 1,25(OH)2D3 receptor level and the heterologous up-regulation of the 1,25(OH)2D3 receptor in clonal osteoblast-like cells. *Calcified tissue international.* **49**, 35–42 (1991).
46. Wang, Y., Zhu, J. & DeLuca, H. F. Identification of the vitamin D receptor in osteoblasts and chondrocytes but not osteoclasts in mouse bone. *J Bone Miner Res.* **29**, 685–692 (2014).
47. Woeckel, V. J. *et al.* 1 α ,25-(OH)2D3 acts in the early phase of osteoblast differentiation to enhance mineralization via accelerated production of mature matrix vesicles. *J Cell Physiol.* **225**, 593–600 (2010).
48. van Driel, M. *et al.* Evidence that both 1 α ,25-dihydroxyvitamin D3 and 24-hydroxylated D3 enhance human osteoblast differentiation and mineralization. *J Cell Biochem.* **99**, 922–935 (2006).
49. Goebel, S. *et al.* FGF23 is a putative marker for bone healing and regeneration. *J Orthop Res.* **27**, 1141–1146 (2009).
50. Sato, Y. *et al.* Changes in bone and calcium metabolism following hip fracture in elderly patients. *Osteoporos Int.* **12**, 445–449 (2001).
51. Hitz, M. F., Jensen, J. E. & Eskildsen, P. C. Bone mineral density and bone markers in patients with a recent low-energy fracture: effect of 1 y of treatment with calcium and vitamin D. *Am J Clin Nutr.* **86**, 251–259 (2007).
52. Yu-Yahiro, J. A. *et al.* Serum and urine markers of bone metabolism during the year after hip fracture. *J Am Geriatr Soc.* **49**, 877–883 (2001).
53. Dirschl, D. R., Henderson, R. C. & Oakley, W. C. Accelerated bone mineral loss following a hip fracture: a prospective longitudinal study. *Bone.* **21**, 79–82 (1997).
54. Lyles, K. W., Schenck, A. P. & Colon-Emeric, C. S. Hip and other osteoporotic fractures increase the risk of subsequent fractures in nursing home residents. *Osteoporos Int.* **19**, 1225–1233 (2008).
55. Pisani, P. *et al.* Major osteoporotic fragility fractures: Risk factor updates and societal impact. *World J Orthop.* **7**, 171–181 (2016).
56. Haffner-Luntzer, M. *et al.* Inhibition of Midkine Augments Osteoporotic Fracture Healing. *PLoS One.* **11**, e0159278 (2016).
57. Bouxsein, M. L. *et al.* Guidelines for assessment of bone microstructure in rodents using micro-computed tomography. *J Bone Miner Res.* **25**, 1468–1486 (2010).
58. Dempster, D. W. *et al.* Standardized nomenclature, symbols, and units for bone histomorphometry: a 2012 update of the report of the ASBMR Histomorphometry Nomenclature Committee. *J Bone Miner Res.* **28**, 2–17 (2013).
59. Busse, B. *et al.* Increased calcium content and inhomogeneity of mineralization render bone toughness in osteoporosis: mineralization, morphology and biomechanics of human single trabeculae. *Bone.* **45**, 1034–1043 (2009).
60. Koehne, T. *et al.* Trends in trabecular architecture and bone mineral density distribution in 152 individuals aged 30–90 years. *Bone.* **66**, 31–38 (2014).
61. Haffner-Luntzer, M. *et al.* Midkine-deficiency delays chondrogenesis during the early phase of fracture healing in mice. *PLoS One.* **9**, e116282 (2014).

Acknowledgements

We wish to thank the German Research Foundation (CRC1149) for supporting this study. We also thank Iris Baum, Sevil Essig, Uschi Maile, Stefanie Schroth and Marion Tomo for excellent technical assistance. This work was supported by the German Research Foundation in the framework of the Collaborative Research Centre 1149 (CRC1149) “Danger response, disturbance factors and regenerative potential after acute trauma”.

Author Contributions

Study design: V.F., M.H.L., T.S., M.A. and A.I. Study conduct: V.F. and K.P. Data collection: V.F., K.P. and A.v.S. Data analysis: V.F. and A.v.S. Data interpretation: V.F., M.H.L., A.v.S., B.B., T.S., M.A. and A.I. Drafting manuscript: V.F., M.H.L. and A.I. Revising manuscript content: V.F., M.H.L., K.P., A.v.S., B.B., T.S., M.A. and A.I. Approving final version of manuscript: V.F., M.H.L., K.P., A.v.S., B.B., T.S., M.A. and A.I. V.F. and A.v.S. take responsibility for the integrity of the data analysis.

Additional Information

Supplementary information accompanies this paper at doi:[10.1038/s41598-017-07511-2](https://doi.org/10.1038/s41598-017-07511-2)

Competing Interests: The authors declare that they have no competing interests.

Publisher's note: Springer Nature remains neutral with regard to jurisdictional claims in published maps and institutional affiliations.



Open Access This article is licensed under a Creative Commons Attribution 4.0 International License, which permits use, sharing, adaptation, distribution and reproduction in any medium or format, as long as you give appropriate credit to the original author(s) and the source, provide a link to the Creative Commons license, and indicate if changes were made. The images or other third party material in this article are included in the article's Creative Commons license, unless indicated otherwise in a credit line to the material. If material is not included in the article's Creative Commons license and your intended use is not permitted by statutory regulation or exceeds the permitted use, you will need to obtain permission directly from the copyright holder. To view a copy of this license, visit <http://creativecommons.org/licenses/by/4.0/>.